JOURNAL OF Applied Polymer SCIENCE

An Easy Method for the Preparation of Anion Exchange Membranes: Graft-Polymerization of Ionic Liquids in Porous Supports

Géraldine Merle, Annisa Chairuna, Erik Van de Ven, Kitty Nijmeijer
Membrane Science & Technology, Mesa+ Institute for Nanotechnology, University of Twente,
7500 AE Enschede, The Netherlands
Correspondence to: K. Nijmeijer (E-mail: d.c.nijmeijer@utwente.nl)

ABSTRACT: A novel way for anion exchange membrane (AEM) preparation has been investigated, avoiding the use of expensive and toxic chemicals. This new synthetic approach to prepare AEMs was based on the use of a porous polybenzylimidazole membrane as support in which functionalized ILs were introduced and subsequently grafted on the polymer backbone. These new AEMs were prepared and their chemical structures and properties including morphology, thermal stability, and ionic conductivity were characterized. The hydroxyl ionic conductivity of the synthesized membranes can reach values upto 6.62×10^{-3} S cm^{-1} at 20°C. Although the ionic conductivity is not very high yet, the work shows the strength of the concept. Membrane properties can be easily tailored toward specific applications by choosing the proper chemistry, i.e., porous polymer support, ionic liquid, and method of initiation and polymerization. © 2012 Wiley Periodicals, Inc. J. Appl. Polym. Sci. 129: 1143–1150, 2013

KEYWORDS: grafting; ionic liquids; membranes

Received 17 September 2012; accepted 3 November 2012; published online 26 November 2012
DOI: 10.1002/app.38799

INTRODUCTION

Recent years have shown extensive research on the preparation, characterization, and application of anion exchange membranes (AEMs).[1] Such AEMs usually contain positively charged groups, such as $-NH_3^+$, $-NRH_2^+$, $-NR_2H^+$, $-NR_3^+$, $-PR_3^+$, $-SR_2^+$, etc., anchored to the polymer backbone, allowing the passage of anions while repelling cations. Today, these AEMs are an essential and an integral part of, e.g., fuel cell technology[2] and daily processes that require the separation of liquid mixtures or gases.[3] AEMs are commercially available and used in chemical and biomedical industries as well as in water desalination and wastewater purification.[3] Over the last 50 years, the demand for AEMs has been steadily increasing and is set to increase in the near future with the development of large scale applications such as salinity gradient energy[4] and alkaline fuel cell technology.[2] Consequently, there is an extensive interest in sustainable and environmentally friendly technologies for the development of AEMs.

Contrary to their acidic homologous the cation exchange membrane, AEM technology is still in its early stages of development, and significant improvements need to be achieved in their preparation for a successful large scale implementation. A large number of papers in literature describe the preparation and use of polymers with tethered cationic groups. For instance, Varcoe et al., report a noticeable AEM system based on quaternary ammonium-functionalized radiation-grafted poly(ethylene-*co*-tetrafluoro ethylene) (ETFE).[5,6] The resulting membranes exhibited significant conductivities up to 34×10^{-3} S cm^{-1} at 50°C. However, the production of such membranes at a large scale is expensive and physically impracticable due to the use of electron beam technology used for irradiation. Another way to introduce cationic moieties into a polymer such as polystyrene,[7] poly(ether imide),[8] poly(*p*-phenylene oxide),[9] or polysulfone,[10] is via chemical modification. Fang and Shen synthesized AEMs by introducing chloromethyl groups and subsequently quaternary ammonium groups into poly(phtalazinone ether sulfone ketone) (PPESK).[11] The results showed a potential of these membranes for use in AEM fuel cells because of the high thermal stability and good ionic conductivity (i.e., 5×10^{-3}–140×10^{-3} S cm^{-1} depending on the concentration of the KOH solution). However, the introduction of the functional group on the polymer backbone suffers from the use of chloromethylmethyl ether, known as carcinogenic. Another possibility to introduce a functional group on an aromatic polymer such as poly (*p*-phenylene oxide)[9] is to brominate the methyl group at the benzene ring by using bromine instead of the highly carcinogenic chloromethyl methyl ether. However, special care needs to be taken when transporting and using bromine since the released gas is highly toxic. Consequently, there exists a clear and crucial need for alternative, easy, and

Applied Polymer SCIENCE

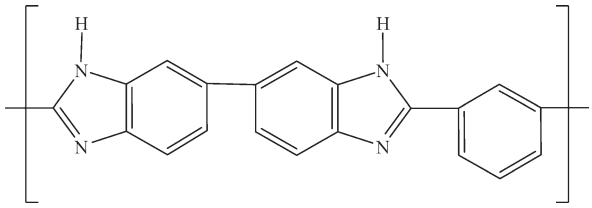

Figure 1. Repeating unit of PBI.

nontoxic paths to affordable AEM preparation. Based on this, we have developed a new way to synthesize AEMs, free of toxic and expensive materials, that in the future is commercially and practically up scalable.

Polybenzimidazole [PBI, poly(1,4-phenylene-5,5 (6-bibenzimidazole-2,2–diyl)), Figure. 1] is a well-known polymer for its high thermal and chemical stability showing a great potential in PEMFC applications.[12] PBI was often doped with phosphoric acid to promote proton conductivity. This non water-soluble polymer exhibits excellent durability, both in alkaline media and at high temperature.[13] Due to two imidazole groups in one repeat unit, this weakly basic polymer is an electronic and ionic insulator. Moreover, the —NH— and —N= groups present at the imidazole rings allow the introduction of cationic moieties at the polymer backbone, necessary for the ionic transport.

ILs have been recently attracting attention. The extremely low vapour pressure of ionic liquids prevents evaporation and they are frequently characterized as 'green solvents'. Next to their low volatility, these materials offer other precious and unique properties such as high ion conductivity, nonflammability, and thermal stability over a wide temperature range.[14] Consequently their potential application is their use as new types of electrolytes in several electrochemical processes.[15,16] For instance, many studies in the field of electrochemical capacitors and lithium batteries indicate that ILs offer tremendous promise to act as ionic conductive materials.[17] In fuel cell applications, recently some studies on the use of ILs in fuel cells have been published, and promising results are described.[18] De Souza et al.[19] developed a system based on IL impregnated membranes. Their work revealed a maximum power density of 1.75×10^{-3} W cm^{-2}.[19] Others report the use of polymeric ionic liquid membranes[20–22] containing imidazolium, tetraalkylammonium, etc. Nevertheless, these membranes still suffer from a poor ionic conductivity and especially a very poor mechanical stability due to leaching out of the IL.

Combining the excellent ion conductive properties of ILs with the high stability of PBI appears a very promising approach to prepare AEMs in a simple way, avoiding the use of toxic chemicals and fastidious preparation. We use tailor-made porous PBI membranes that we fill with the selected IL. Subsequently the IL is chemically immobilized onto PBI via a graft-polymerization. This method is expected to significantly increase the ionic conductivity of the PBI membrane while keeping its excellent mechanical and chemical stability, as leaching out is restricted due to the chemical bond between the IL and PBI. 2-(Methacryloyloxy) ethyl trimethyl ammonium] chloride (MTAC) was chosen as the ionic liquid because of its methacryloyloxy function allowing the graft-polymerization, its low cost, and its absence of toxicity.

Here, we investigate two aspects of the preparation of these membranes: (1) the incorporation and the grafting of the IL inside PBI membranes and (2) the influence of the incorporation and grafting of IL in the PBI membrane on the ionic conductivity, water uptake, and thermal stability of the membrane for potential application as polymer electrolyte membrane.

EXPERIMENTAL

Materials

Ultrahigh molecular weight PBI polymer powder (FumaTech BmbH), 1-methyl-2-pyrrolidinone (NMP, 99% Acros Organics), ethanol (Merck), *n*-hexane (Merck), lithium chloride anhydrous (LiCl, Sigma-Aldrich), poly (vinyl pyrrolidone) K30 (PVP K30, Fluka), poly (vinyl pyrrolidone) K90 (PVP K90, Fluka), the ionic liquid [2-(methacryloyloxy) ethyl trimethyl ammonium] chloride (MTAC, 80% wt % solution in water, Sigma-Aldrich), benzoyl peroxyde (BPO, 98% Sigma-Aldrich), and toluene (Merck) were purchased and used as received.

Membrane Preparation

Porous PBI Membrane. The preparation of pristine porous PBI was carried out using a slow phase inversion method. A homogenous polymer solution was prepared by mixing ultrahigh molecular weight PBI (12 g), PVP K30 (2 g), PVP K90 (2 g), and LiCl (2 g) in 2182 mL of NMP solvent. LiCl was added to stabilize the polymer solution,[23] while the addition of PVP suppresses the macrovoid formation in the membrane and improves the casting properties.[24,25] The mixture was heated up to 175°C at constant stirring for 24 hours using a conical flask attached to a reflux condenser. The resulting polymer solution was filtered under air pressure through a 25 μm metal filter type ST 15 AL 3 (Bekeart) to finally obtain a high viscosity polymer solution. This polymer solution was slowly casted onto a glass plate using a 0.15 mm casting knife at room temperature. The casted membrane was immediately immersed in a coagulation solution of H_2O/NMP (1 : 1) for 30 minutes resulting in a brownish membrane. To remove remaining traces of solvent, the membrane was soaked in ultrapure water for 30 minutes. To avoid brittleness and curling of the membrane, the membrane was dried via solvent exchange in a stepwise transition from a polar to a nonpolar solvent. First, water was removed out of the membrane by immersing the membrane in a pure methanol bath for 30 minutes. After that, the membrane was subsequently dipped in pure *n*-hexane for 30 minutes to remove the methanol. Finally, the membrane was dried between tissue pape,r and the residual solvent was removed by drying the membrane in an oven at 150°C overnight.

Introduction of Cationic Moieties. The porous PBI membrane was placed and glued at the sides on a perforated aluminium plate using double-sided tape. The backside of the plate supporting the membrane was connected to a vacuum pump to create a vacuum over the membrane to facilitate the impregnation of the ionic liquid MTAC into the porous PBI (Figure. 2). MTAC (100 μL/cm^2) was dropped slowly on the membrane surface until it was fully covered and sucked into the membrane for ~ 15 min.

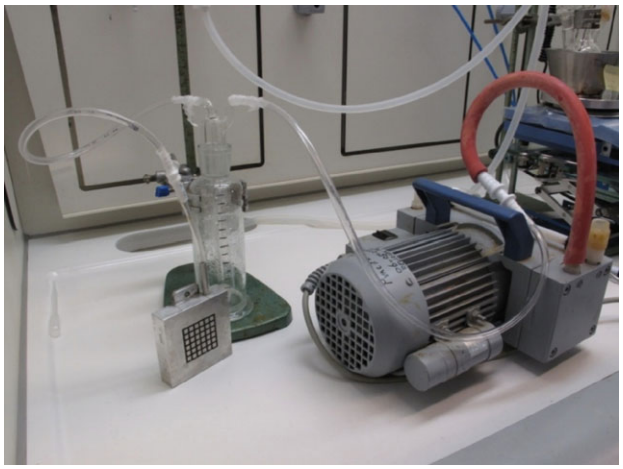

Figure 2. Picture of the setup used to impregnate the porous PBI membrane. [Color figure can be viewed in the online issue, which is available at wileyonlinelibrary.com.]

Subsequently, the membrane was placed in a three-necked flask containing BPO (0.01*M*) in toluene at 85°C under reflux and a nitrogen atmosphere to graft the ionic liquid MTAC onto the PBI backbone according to the synthetic route described in Figure 3. After 1 hour, the membrane was rinsed with water and ethanol for three times during 30 minutes respectively, to remove the unreacted ionic liquid monomer and the undesirable ionic liquid homopolymer. This whole procedure was repeated two times.

Alkalization. After the graft polymerization procedure, the MTAC-PBI membrane appears in the Cl^-form. To convert the membrane from its Cl^- into its OH^- form, the membrane was immersed in 1*M* NaOH solution for 20 minutes at room temperature. To remove the formed NaCl and to neutralize the membrane, the membrane was subsequently rinsed with ultrapure water until the pH of the water remained neutral.

Membrane Characterization

Volume Porosity. A Micrometrics pycnometer model ACCUPYC 1330 was used to determine the volume porosity of the prepared PBI supports and the PBI/IL membranes. The measurement was based on Archimedes' displacement principle, and the sample volume was determined by measuring the pressure change of helium in a calibrated volume. The method is described elsewhere.[26] For each experiment 10 samples were measured.

Fourier Transform Infrared Spectroscopy (FTIR). The chemical structure of the membrane was analyzed by Fourier Transform Infra-Red Spectroscopy (FTIR) using a Perkin Elmer Fourier Transform Infrared Spectroscope 1000. The measurements were performed using KBr. The FTIR spectra were recorded in the range from 4000 to 400 cm^{-1} with four scans at a resolution of 4.0 cm^{-1}.

Scanning Electron Microscopy (SEM). The geometrical characteristics and the morphology of the developed membranes were determined using a Jeol JSM-T220 scanning electron microscope. Membrane samples were fractured in liquid nitrogen and sputtered with a thin layer of gold using a Balzers Union SCD 040 sputtering apparatus. Membranes were examined at magnifications of 1000×, 2500× and 8000×.

Thermal gravimetric analysis (TGA). TGA analysis was carried out using a Perkin Elmer TGA 7 system. Samples were heated from 50°C to 700°C under nitrogen atmosphere at a heating rate of 20°C min^{-1}.

Water Uptake. The dry membrane (weight W_d) was immersed in an excess amount of deionized water at ambient temperature until saturation, which was reached when a constant weight was obtained. The weight of the wet membrane (weight W_w) was measured after gentle removal of the remaining surface water with blotting paper. The water uptake (WU) was subsequently calculated using the following formula:

$$\mathrm{WU} = \left[\frac{(W_w - W_d)}{W_d}\right] \times 100\% \quad (1)$$

All measurements were performed four times.

Ionic Conductivity. The hydroxyl conductivity of the membrane was determined using impedance spectroscopy in a homemade cell.[27] The cell has a Teflon interior with two circular platinum electrodes and a surface area of 0.785 cm^2. Both electrodes were connected with two wires, one to carry the current and one to act as potential probe. The cell was connected to a frequency response analyzer (FRA-Autolab). The membrane sample was sandwiched between the platinum electrodes and the resistance through the plane was measured. The impedance spectrum was recorded in the frequency range from 0.1 Hz to 104 KHz at a potential amplitude of 0.01 V at room temperature using a PGstat20 Autolab Potentiostat with integrated frequency response analyzer (ECO-Chemie, The Netherlands). The ionic conductivity was calculated based on the average of four different samples using eq. (2)

$$\sigma = \frac{l}{R.A} \quad (2)$$

where σ is the OH^- conductivity of the membrane (S/cm), l is the thickness of the membrane (cm), R is the membrane resistance (σ), and A is the surface area of the electrodes (cm^2). Prior to each measurement, the membrane was immersed in water at room temperature and the surface water was gently removed using blotting paper. The water content of the swollen membrane was assumed to remain constant during the short period of time required for the measurement.

RESULTS AND DISCUSSION

Membrane Preparation

The prepared membrane is denoted as [MTAC-PBI][OH^-]. The membrane is brownish and can be easily bended or cut into any desired size and shape. This is in contrast to the pristine PBI membranes, which need to be handled with care due to their brittleness.

Volume Porosity and Gravimetric Analysis. To validate this new approach to prepare stable anion exchange membranes and to optimize the number of impregnation/polymerization cycles required, the weight of the membrane, and the volume

Applied Polymer SCIENCE

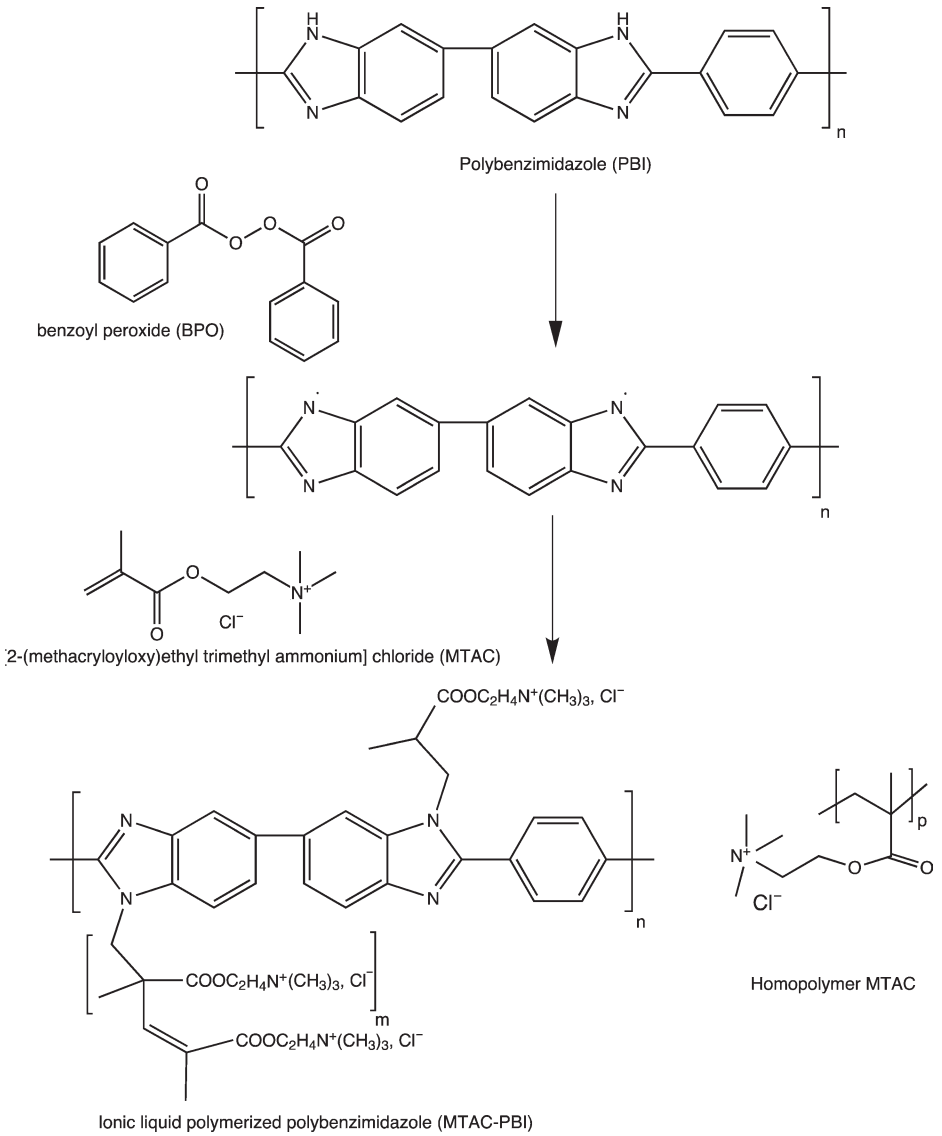

Figure 3. Mechanism of graft polymerization of the IL MTAC onto the PBI polymer backbone.

porosity of the native PBI membrane and the [MTAC-PBI][Cl^-] grafted membranes were determined as a function of the number of impregnation cycles. The measurements were done directly after every single cycle. The results are summarized in Figure 4.

When introduced in the pores of the porous PBI membrane, the ionic liquid MTAC fills the pores of the membrane and consequently, the weight of the membrane increases and its volume porosity decreases. Figure 4 shows that the weight of the [MTAC-PBI][Cl^-] grafted PBI membrane increases gradually after the first and second cycle. A maximum weight increase of 100% is observed after the second cycle combined with a decrease of the volume porosity to only 25%. Only a minor decrease in weight and corresponding change in volume porosity is observed after the third cycle. However, these variations are within the experimental error of the experiments. We assume that at this stage, the two previous cycles of impregnation/polymerization decreased the porosity of the membrane

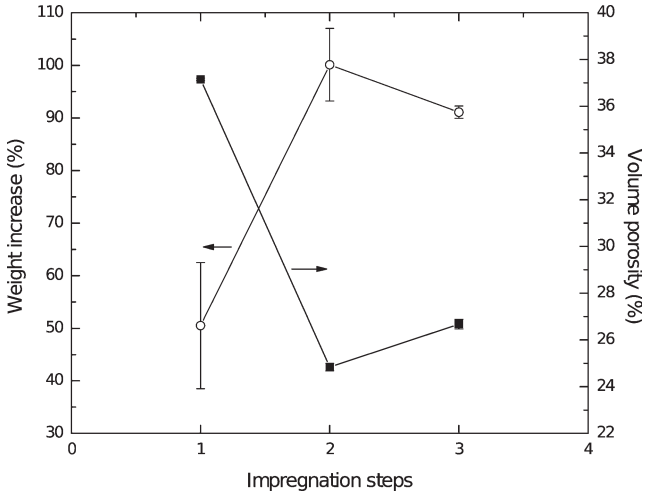

Figure 4. Relative weight increase and volume porosity of the [MTAC-PBI][Cl^-] grafted membrane versus the number of impregnation cycles.

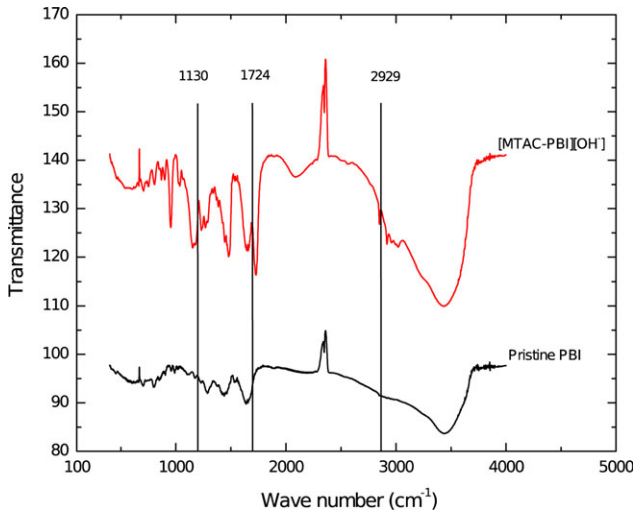

Figure 5. FTIR spectra of pristine PBI and the [MTAC-PBI][OH^-] impregnated membrane. [Color figure can be viewed in the online issue, which is available at wileyonlinelibrary.com.]

and therefore further impregnation is not possible anymore, as the monomer is not able to diffuse inside the membrane pores and subsequently to polymerize. Based on the weight increase of the membrane after each cycle, we were able to estimate the amount of MTAC introduced into the porous PBI. After the first and the second cycle, an amount of 1.84×10^{-4} and 2.87×10^{-4} mol of MTAC was introduced respectively.

The maximum weight increase is obtained after the second impregnation cycle. At this stage also the volume porosity has reached its lowest value. More impregnation steps do not have any additional value, as both the weight and the porosity of the membranes do not change significantly anymore. This indicates that two cycles are sufficient to fill the majority of the void fraction of the porous membrane with the conductive ionic liquid. Consequently, only these membranes were subject to further investigations.

FTIR. Fourier transform infrared (FT-IR) spectra of pristine PBI and [MTAC-PBI][OH^-] grafted membranes were recorded and shown in Figure 5.

Figure 5 depicts the characteristic peaks of the pristine PBI. The breathing mode of the imidazole ring is visible at 1296.5 cm^{-1}. The other peaks represent C—C stretching and C—H stretching of the aromatic groups of the PBI. The FTIR spectrum of the [MTAC-PBI][OH^-] grafted membrane exhibit several characteristic peaks at 2929, 1724, and 1130 cm^{-1}, which correspond to stretching of the N^+—C, C=O and C—O—C (ether) linkage, respectively.[28] These bonds are the characteristic structural features of MTAC present in the PBI membrane. Taking into account that the membranes were rigorously rinsed in ethanol and water to remove the unreacted ionic liquid, these results show that MTAC was successfully introduced and grafted into the PBI membrane.

SEM. The morphology of pristine PBI and the [MTAC-PBI][OH^-] grafted membrane was characterized using scanning electron microscopy (SEM). Figure 6 shows that the pristine PBI membrane exhibits a highly porous structure. This in contrast to the [MTAC-PBI][OH^-] grafted membrane, which has a dense, homogenous and uniform surface without pores.

Figure 7 shows the SEM pictures of the cross sections of (a) the pristine PBI and (b) the [MTAC-PBI][OH^-] grafted membrane (b). The cross section of the pristine PBI membrane shows a porous structure. The [MTAC-PBI][OH^-] grafted membrane, in contrast, is dense without any visible pores throughout the cross section of the membrane. The thickness of the pristine PBI membrane and the [MTAC-PBI][OH^-] grafted membrane as estimated from the SEM images is ~48 and 66 μm, respectively. This increase in thickness is due to the insertion of MTAC in but also to a small extent on top of the PBI membrane. We hypothesize that the radical created at the PBI is transferred to the MTAC monomer units present inside the membrane but also to those present at the surface of the membrane. Once the MTAC has been anchored onto the PBI backbone, the MTAC chains continue to grow as long as long there is MTAC monomer present. Consequently, we expect that next to grafting and polymer chain growth inside the pores we expect also some growth on the surface of the membrane, leading to an increase in the membrane thickness. These results are confirmed by the fact that the maximum degree of impregnation is obtained after two impregnation steps.

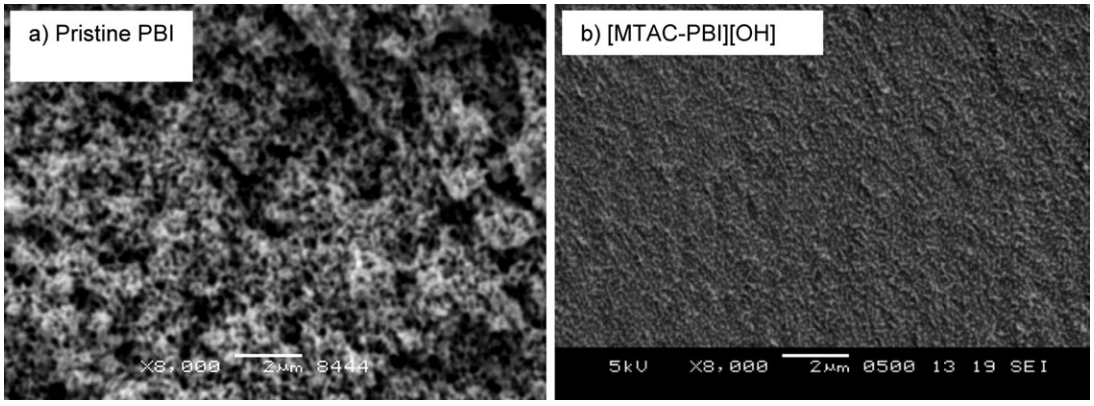

Figure 6. SEM picture of surface of (a) the pristine PBI and (b) the [MTAC-PBI][OH] grafted membrane at a magnification of 8000×.

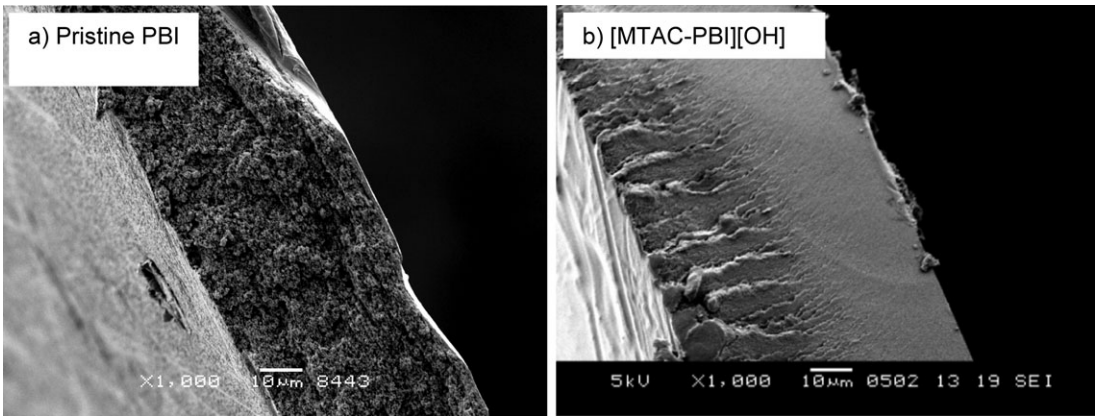

Figure 7. SEM picture of the cross section of (a) the pristine PBI and (b) the [MTAC-PBI][OH^-] grafted membrane at a magnification of 1000×.

TGA. The temperature stability of the developed membranes was addressed using thermal gravimetric analysis (TGA). Figure 8 shows the thermogravimetric data of pristine PBI and those of the [MTAC-PBI][OH^-] grafted membrane.

Within the experimental error of the system, pristine PBI shows a weight loss of ~10 wt % up to 150°C, corresponding to the evaporation of absorbed water. From 150°C to 300°C, no further significant weight loss is recorded, showing the excellent thermal stability of this polymer. The [MTAC-PBI][OH^-] membrane shows distinct areas of weight loss. A first weight loss of ~ 6 wt % up to 150°C is visible, which is attributed to the evaporation of water. The second weight loss observed at temperatures above 230°C may be due to the degradation of the tetraalkyl ammonium cations of the MTAC.[29]

Ionic Conductivity and Water Uptake. The high ionic conductivity of the membranes can be improved by increasing the amount of charged groups in the membrane. However, this usually coincides with a loss of the mechanical properties because of excessive water uptake. On the other hand, membranes in the dry state are often brittle and show low conductivities, like pristine PBI. Both excessive swelling and brittleness have a negative impact on the fuel cell performance. Figure 9 shows the ionic conductivity and the water uptake of the [MTAC-PBI][Cl^-] membranes versus the number of impregnation cycle. Together these values give an indication about the number of charged groups in the membranes.

The results show that the ionic conductivity as well as the water uptake increase with the number of impregnation/polymerization cycles. In the first cycle, the ionic conductivity of the [MTAC-PBI][Cl^-] membrane increases from 0.14 × 10^{-3} S cm^{-1} (conductivity of the native PBI membrane) to 3.32 × 10^{-3} S cm^{-1} combined with an increase in the water uptake to a value of 58%. After the second cycle, the [MTAC-PBI][Cl^-] membrane exhibits a significant ionic conductivity of 5.83 × 10^{-3} S cm^{-1} as well as a water uptake of 102.74%. The pristine PBI membrane is hydrophobic and considered as an ionic insulator. Therefore, this increase in both ionic conductivity and water uptake is related to the incorporation of MTAC inside the PBI matrix.

The increase in the amount of MTAC inside the PBI membrane induces an increase in the number of charge carriers, hence, the ionic conductivity of the membrane increases. Moreover, the

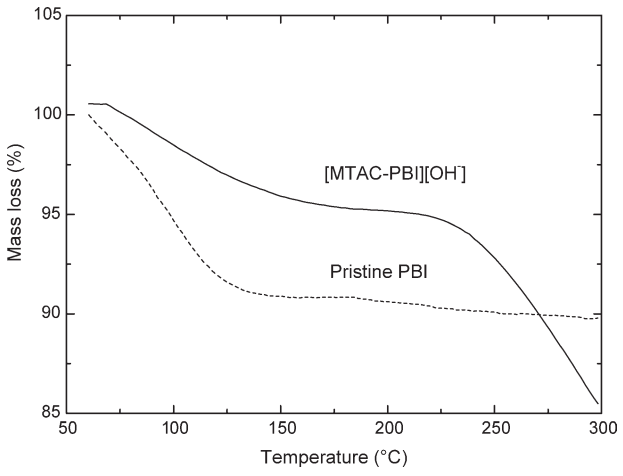

Figure 8. Thermogravimetric analysis of the pristine PBI membrane and the [MTAC-PBI][OH^-] grafted membrane.

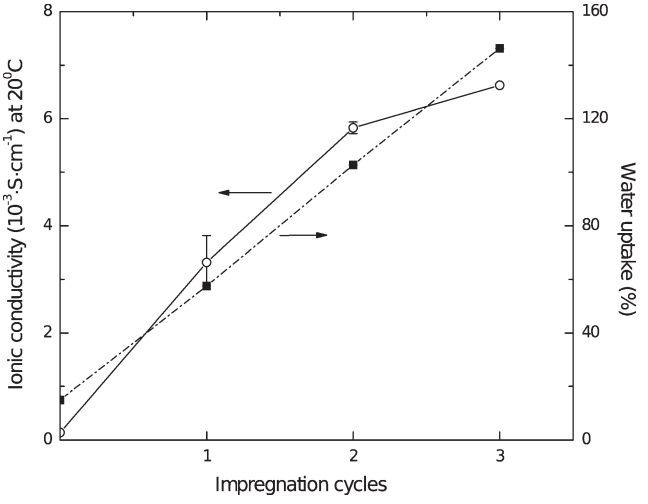

Figure 9. Ionic conductivity and water uptake at 20°C versus the number of impregnation cycles of the [MTAC-PBI][Cl^-] membranes.

MTAC modifies the hydrophobicity of the PBI membrane, making the membrane more hydrophilic and subsequently allowing the presence of water into the membrane. The presence of water in the membrane increases the ionic conductivity by enhancing the mobility of the ions.

After the third cycle, the ionic conductivity only slightly increased from 5.83×10^{-3} S cm^{-1} to 6.62×10^{-3} S cm^{-1}, while the water uptake still significantly increased from 103% to 147%. Literature[2] shows that excessive water uptake can have an opposing effect on the ionic conductivity as it reduces the fixed charge density i.e., the concentration of fixed charged groups in the membrane. The resistance and ionic conductivity of the membrane is determined by the charge density. Consequently the ionic conductivity is a function of both the number of charge carriers and water uptake.

These results for the ionic conductivity were obtained for membranes in the Cl^- form. As in many applications, the membrane will be in its OH^- form, the ionic conductivity of the membranes in their OH^- form was also evaluated. The conversion of the membrane from the Cl^- into the OH^- form was achieved by immersion of the [MTAC-PBI][Cl^-] membranes obtained after two cycles in 1*M* NaOH for 20 minutes at room temperature. After alkalization, we observed a significant increase of the ionic conductivity for the [MTAC-PBI][OH^-] membranes and obtained a value of 10.58×10^{-3} S cm^{-1}. The same conductivity was found for membranes that were immersed longer in the NaOH solution, showing that an immersion time of 20 minutes is sufficient for complete exchange of Cl^- by OH^-.

The chemical stability of anion exchange membranes to withstand especially high pH for alkaline fuel cells is one of fundamental properties of the polymer electrolyte. The stability of the polymer backbone and especially that of the cationic groups is crucial since their degradation will directly affect the ionic conductivity and so the performance of the fuel cells for instance. The chemical stability was evaluated by immersing the membrane in concentrated potassium hydroxide solutions (up to 10*M*) for 25 hours. Although there was almost no change in membrane appearance and no significant change in weight of the membrane, we observed a decrease in ionic conductivity, representative for the loss of the chemical stability of the membrane. This is attributed to the chemical degradation of the alkyl quaternary ammonium polymers, probably caused by an oxygen or hydroxyl attack.[30] Indeed, literature[31] shows that the alkyl quaternary ammonium functionalized polymers are less stable in a concentrated potassium or sodium hydroxide solution due to the displacement of the quaternary ammonium groups by OH^- anions via (i) a direct nucleophillic displacement and/or (ii) a Hofmann elimination reaction when β-hydrogens are present.[2] This causes the loss of the quaternary ammonium groups and therefore influences negatively the ionic conductivity of the membrane. Although the degradation process of the membrane depends on the concentration of KOH in the solution, the membranes exhibit a reasonable tolerance toward base treatment since after 25 hours 40% of the initial ionic conductivity still remained.

We truly believe that this new method will tackle some of the majors issues related to the preparation of AEMs not only in terms of toxicity but also regarding cost and easiness. Another advantage of this method is its flexibility. The technique can be adjusted to a wide range of applications from desalination to fuel cell for instance. This can be easily achieved by adjusting the porous membrane, the ionic liquid and finally the initiation type for polymerization (e.g ionization, persulfate). In the future, we first envisage improving this method and then to further explore this new concept. For instance we considered to develop and investigate a series of other cationic groups, such as *N*-alkyl-substituted imidazolium cations, which are expected to show superior chemical and thermal stability compared to the quaternary ammonium entities[32] and to apply these new materials in different types of processes. We are fully convinced that this simple technique is not only an important progress in the preparation of anion exchange membranes but also for the development of other more advanced functional membranes.

CONCLUSIONS

A novel path for AEM preparation was investigated offering the possibility to work without the use of expensive and toxic compounds. This new synthetic approach to prepare AEMs was based on the use of a porous polybenzylimidazole membrane as support in which functionalized ILs were introduced and subsequently grafted on the polymer backbone. These new AEMs were prepared and their chemical structures and properties including morphology, thermal stability, and ionic conductivity were characterized. The hydroxyl ionic conductivity of the synthesized membranes can reach values up to 6.62×10^{-3} S cm^{-1} at 20°C. Thermal gravimetric analysis shows that these types of membranes are thermally stable, as only a weight loss up to 150°C was recorded due to the evaporation of water. In the future, we plan to exchange the alkyl quaternary ammonium to imidazolium groups to increase the stability of these new types of membranes in alkaline environment. Although the ionic conductivity is not very high yet, the work shows the strength of the concept. Membrane properties can be easily tailored to wards specific applications by choosing the proper chemistry, i.e. porous polymer support, ionic liquid, and method of initiation and polymerization.

REFERENCES

1. Hideo, K.; Tsuzura, K.; Shimizu, H. In Ion Exchangers; Walter de Gruyter, Dorfner, K., Eds.; Walter de Gruyter, Berlin, **1991**.
2. Merle, G.,Wessling, M.,Nijmeijer, K. *J. Memb. Sci.* **2011**, *377*, 1.
3. Strathmann, H. In Membrane Separation Technology—Principles and Applications; Nobel, R. D., Stern, S. A., Eds.; Elsevier, Amsterdam, **1995**; 214.
4. Długolęcki, P.; Gambier, A.; Nijmeijer, K.; Wessling, M. *J. Environ. Sci. Technol.* **2009**, *43*, 6888.
5. Varcoe, J. R.; Slade, R. C. T. *Electrochem. Commun.* **2006**, *8*, 839.
6. Varcoe, J. R.,Slade, R. C. T., Lam How Yee, E.; Poynton, S. D.; Driscoll, D. J.; Apperley, D. C. *Chem. Mater.* **2007**, *19*, 2686.

7. Dragan, E. S.; Avram, E.; Axente, D.; Marcu, C. *J. Polym. Sci., Part A: Polym. Chem.* **2004**, *42*, 2451.
8. Wang, G.; Weng, Y.; Zhao, J.; Chen, R.; Xie, D. *J. Appl. Polym. Sci.* **2009**, *112*, 721.
9. Li, Y.; Xu, T. *J. Appl. Polym. Sci.* **2009**, *114*, 3016.
10. Zhou, J.; Unlu, M.; Vega, J. A.; Kohl, P. A. *J. Power Sources* **2009**, *190*, 285.
11. Fang, J.; Shen, P. K. *J. Memb. Sci.* **2006**, *285*, 317.
12. Cloe, E. W. Polymer Materials Encyclopedia; CRC Press: New York, **1996**.
13. Chung, T. S. J. *Macromol. Sci. Rev. Macromol. Chem. Phys.* **1997**, *37*, 277.
14. Washiro, S.,Yoshizawa, M.,Nakajima, H.,Ohno, H. *Polymer* **2004**, *45*, 1577.
15. Fuller, J.; Carlin, R. T.; Osteryoung R. A. *J. Electrochem. Soc.* **1997**, *144*, 3881.
16. Fuller, J.; Breda, A. C.; Carlin, R. T. *J. Electroanal. Chem.* **1998**, *459*, 29.
17. Lewandoski, A.; Świderska-Mocek, A. *J. Power Sources* **2009**, *194*, 601.
18. Guo, M.; Fang, J.; Xu, H.; Li, W.; Lu, X.; Lan, C.; Li, K. *J. Memb. Sci* **2010**, *362*, 97.
19. De Souza, R. F.; Padilha, J. C.; Gonçalves, R. S.; Dupont, J. *Electrochem. Commun.* **2003**, *5*, 728.
20. Carlisle, T. K.; Bara, J. E.; Lafrate, A. L.; Gin, D. L.; Noble, R. D. *J. Memb. Sci.* **2010**, *359*, 37.
21. Neves, L. A.; Coelhoso, I. M.; Crespo, J. G. *J. Memb. Sci.* **2010**, *360*, 363.
22. Green, O.; Grubjesic, S.; Lee, S.; Firestone, M. A. *Polym. Rev.* **2009**, *49*, 339.
23. Lin, H. L.; Chen, Y. C.; Li, C. C.; Cheng, C. P.; Yu, T. L. *J. Power Sources* **2008**, *181*, 228.
24. Yoo, S. H.; Kim, J. H.; Jho, J. Y.; Won, J.; Kang, Y. S. *J. Memb. Sci.* **2004**, *236*, 203.
25. Boom, R. M.; Wienk, I. M.; Van Den Boomgaard, T.; Smolders, C. A. *J. Memb. Sci.* **1992**, *73*, 277.
26. Reijerkerk, S. R.; Jordana, R.; Nijmeijer, K.; Wessling, M. *Int. J. Greenhouse Gas Control.* **2011**, *5*, 26.
27. Merle, G.; Hosseiny, S. S.; Wessling, M.; Nijmeijer, K. *J Memb. Sci*, **2012**, *409*, 191.
28. Chowdhury, P.; Mondal, P.; Roy, K. *Polym. Bull.* **2010**, *64*, 351.
29. Ngo, H. L.; LeCompte, K.; Hargens, L.; McEwen, A. B. *Thermochim. Acta.* **2000**, *357*, 97.
30. Xiong, Y.; Liu, Q. L.; Zhang, Q. H.; Zhu, A. M. *J. Power. Sources.* **2008**, *183*, 447.
31. Guo, M.; Fang, J.; Xu, H.; Li, W.; Lu, X.; Lan, C.; Li, K. *J. Membr. Sci.* **2010**, *362*, 97.
32. Sowmiah, S.; Srinivasadesikan, V.; Tseng, M. C.; Chu, Y. H. *Molecules* **2009**, *14*, 3780.
33. Li, X. H.; Zhao, D. B.; Fei, Z. F.; Wang, L. F. *Sci. China Ser. B* **2006**, *49*, 385.
34. Strackea, M. P.; Migliorini, M. V.; Lissner, E.; Schrekker, H. S.; Dupont, J.; Goncalves, R. S. *Appl. Energy*, **2009**, *86*, 1512.